EFFECT OF WIDTH-THICKNESS RATIOS ON THE AXIAL CAPACITY OF STEEL TUBULAR COLUMN FILLED WITH RECYCLED BRICK AGGREGATE CONCRETE

Shams-E-Imrekha Khanam[1], Md. Khasro Miah[*2], A. K. M. Ruhul Amin[3]

[1] PG Student, Dhaka University of Engineering & Technology, Gazipur, Bangladesh,
Email : shekhi.ceduet@gmail.com
[2] Professor, Dhaka University of Engineering & Technology, Gazipur, Bangladesh,
Email : mkhasro@duet.ac.bd
[3] Doctoral Student, Dhaka University of Engineering & Technology, Gazipur, Bangladesh,
Email : akm.ruhul69@gmail.com

***Corresponding Author**

ABSTRACT

Concrete-filled hollow steel tubular (CFHST) columns are largely used accounting for high strength and ductility. CFHST column has become popular and plays an important role in constructions. Stone aggregate concrete was mostly used as infill of CFHST columns. This popularity is owing to its structural behavior viz excellent seismic resistivity properties and large energy absorption capacity. Due to scarcity of natural stone, crushed clay bricks are extensively used in Bangladesh for producing concrete and the mechanical properties of brick aggregate concrete (BAC) has been found quite satisfactory but different from that of SAC especially the modulus of elasticity, the modulus of rupture and shrinkage. Besides this, in many developing countries, such as in India and Bangladesh, bricks are extensively used as the non-structural walls and coarse aggregate in the concrete building. The demolishing of this kind of buildings generates huge waste. Currently, most of the bricks from old demolished buildings are being used by landfills, which are not only wastage of resources but also cause environmental problems. This problem can be minimized using demolished bricks as coarse aggregate as infill concrete of CFHST columns. However, no potential attempts were made to study the axial behavior of CFHST columns filled with recycled brick aggregate concrete (RBAC) so far. In this regard, axial load capacity, load versus deformation behavior and failure behavior of CFHST column specimens were observed both experimentally and numerically. The experimental program consisted of nine CFHST column specimens varying width-to-thickness (b/t=18, 25 and 35) ratios with L/b ratio of 10 and single concrete strength. The specimens have been tested for concentrically applied axial load to observe the ultimate load carrying capacity, load versus deformation characteristics and failure behavior. The axial load carrying capacity increased corresponding to decrease the axial deformation with the increase of b/t ratios.

Keywords: CFHST Column, Recycled Brick Aggregate, Experiment, ANSYS, Numerical Analysis.

1. INTRODUCTION

The concrete-filled hollow steel (CFHS) columns are being used increasingly as one of the essential elements in buildings, bridges and other concrete structures, because of their excellent earthquake-resistant properties like high stiffness, high strength, high ductility and large energy absorption capacity (Ge and Usami, 1994). The steel tube does not only take axial load but also does provide confining pressure to the concrete core, while the concrete core takes axial load and prevents or delays local buckling of the steel tube (Huang et al., 2002). Infill concrete takes the axial compression and hollow steel section takes axial compression and provides confinement for the infill concrete. Since the steel plates provide the confinement for the infill concrete which in turn prevents the inward buckling of the plate there is a mutual enhancement of ductility and strength in CFHS columns (Ge and Usami, 1992). In a thin-walled concrete filled steel tube, when the lateral deformation of the concrete core is restrained by the steel shell, the core is stressed tri-axially and the tube bi-axially. The stress condition in the concrete core is similar to that in the core of a spirally reinforced concrete column (Neogi, 1967). Recycle brick aggregate from non-structural element of demolished building may be used for the preparation of concrete instead of land filling that may causes environment pollution.

Several researches were conducted on the behavior of concrete filled hollow steel (CFHS) columns using recycled concrete or recycled brick aggregate concrete (RBAC) under different perspective Shanmugam et al. (2002), Yang and Han (2006), Chen et al. (2012), , Xiao et al. (2012), Schwerin et al. (2013), Mohammed et al. (2015), Akhtar and Sarmah (2018), Yuan et al. (2019), Ahmed et al. (2020), and Pandulu et al. (2020) are the many more researchers conducted their researches with recycled concrete or RBAC either in CFHS column specimen or purposes. In all cases of research with CFHS column specimens, found partially replacement of stone aggregate or virgin brick aggregate. However, the research work on the behavior of CFHS columns filled with 100% recycled brick aggregate concrete (RBAC) is very insignificant.

However, no potential attempts were made to study the axial behavior of CFHT columns filled with recycled brick aggregate concrete (RBAC) so far. However, an investigation of CFHS columns with infill as 100% recycled brick aggregate concrete are insignificant. Therefore, an experimental justification is required to verify the use of RBAC as an alternative to conventional SAC or BAC in CFHT columns. In this study, the behavior of steel tubular columns filled with 100% recycled brick aggregate concrete will be investigated under axial load. Therefore, the aim of this research is to investigate the behavior of recycled brick aggregate concrete (RBAC) filled hollow steel columns under concentric load. The behaviors of recycled brick aggregate concrete (RBAC) filled hollow steel columns have been investigated under axial load in this study.

The compressive strength, modulus of elasticity and Poisson's of RBAC also have been determined for the development of stress-strain constituent model to perform the numerical analysis using ANSYS finite element program. Experimental axial load capacity, axial deformation, stress-strain relationships and buckling behavior of recycled brick aggregate concrete filled hollow steel columns have been investigated under axial loads. Numerical axial load capacity and deformation of model columns under axial loads have also been determined using ANSYS Finite Element program. A comparative study between experimental and numerical results of CFST column specimens with RBAC is executed.

2. EXPERIMENTAL TEST PROGRAM

The test program consisted of nine concrete filled steel tube (CFST) specimens of three different sizes. The CFST specimens was filled with recycled brick aggregate concrete (RBAC) having mix ratio of 1:1½:3. These test specimens were square in different size and constructed using same thicknesses steel plates. These specimens were tested under concentric axial load to observe load deformation behavior, ultimate load carrying capacity and the failure behavior. Figure. 1 shows the typical 3-D view and cross-section of HST and CFST test specimens. The geometric parameters illustrated in Figure1(b) and 1(c) are the specimen depth or breadth b, tube thickness t, and the other elements used for the preparation of column CFST specimens. The geometric properties of test specimens with recycled brick aggregate concrete are given in Table 1. Nine CFST test specimens in three different groups were tested under concentric axial load.

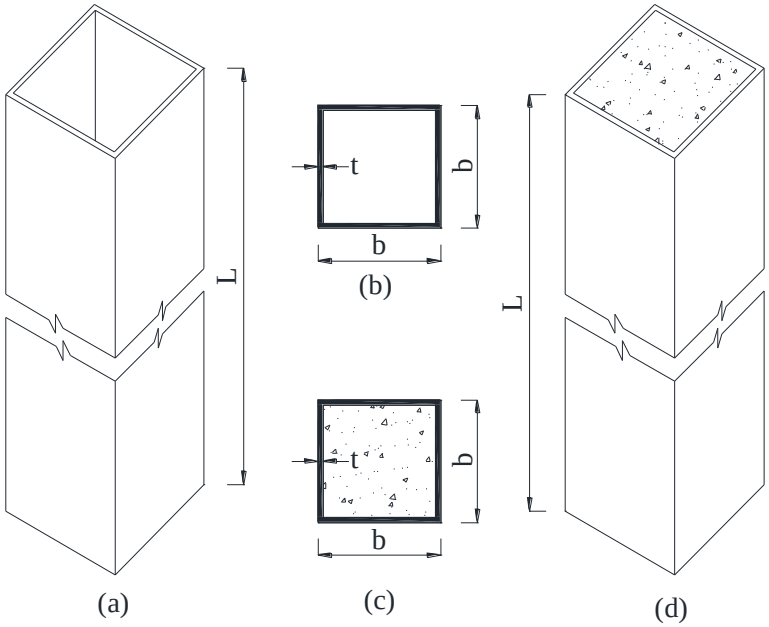

Figure 1: Geometry of CFST test specimens, (a) Hollow Steel Tube (HST), (b) Cross-section of HST, (c) Cross-section of CFST, and (d) Concrete Filled Steel Tube (CFST)

3. MATERIAL PROPERTIES

Locally available Portland composite cement (Shah Cement) was used in this study to prepare the concrete mixture. The cement contains 35 to 40 percent lime, 40 to 50 percent alumina, up to 15 percent iron oxides, and preferably not more than about 6 percent silica. The principal cementing compound is calcium aluminate ($CaO.Al_2O_3$). Physical properties of cement such as normal consistency 29%, specific gravity 3.09, fineness 85.6%, final setting time 1h 48sec., and compressive strength of cement after 28 days 29.9MPa. Well burnt first class recycle bricks were collected from old building to prepare crushing strength test. Standard test method ASTM_C67 (2003) was followed for crushing strength and water absorption of brick 16.3Mpa and 14.9%. The recycled bricks were broken manually using steel hammer to get the required brick chips, Samples passing through ASTM

12.5mm sieve and retained on 4.75mm sieve were used as coarse aggregate. The unit weight and Loss Angeles Abrasion (LAA) value were was 1031 Kg/m^3 and 36%.
Water Absorption capacity was 20.1%, Bulk Specific Gravity was 1.68 (OD) and 2.10 (SSD), Fineness Modulus (FM) and Aggregate Crushing Value were 6.42 and 39.9%. Locally available coarse sand was used for the preparation of concrete. The bulk density and fineness modulus of course sand are 1.67 g/cm3 and 2.80 respectively.

3.1 Steel Material Property

Locally available steel tube with different size and plate thickness was used in this study. This steel tubes were constructed by pressing plane steel plates using a hydraulic press machine. ASTM A36 steel Tube used in this study; this steel tube is available in our local market. For steel plate tensile strength test, three steel plate coupon sample for 2mm thickness plate had been prepared for the test. An average result of yield strength (f_y) found 309MPa. An average ultimate strength (f_u) found 365MPa. This plate tensile test had been conducted in the materials testing laboratory.

Table 1: Geometric Properties of the Test Specimens

Sl. No	Specimen Designation	Steel Tube Size b×b (mm×mm)	Tube Thickness t (mm)	Tube Length L(mm)	b/t Ratio	L/b Ratio
1	FRB-18-10	37.5×37.5	2.0	375	18	10
2	FRB-25-10	50×50	2.0	500	25	10
3	FRB-35-10	70×70	2.0	700	35	10

3.2 Concrete Material Property

Recycle brick aggregate concrete was used in this study. The aim of using recycle brick aggregate to prepare low strength concrete having mix ratio of 1:1½:3. The size of coarse aggregate was ¾ down grade and the fineness modulus (FM) of sand taken 2.50. Locally available cement is used in this test program. Shah cement was used in this study. Three concrete cylinders were constructed in each batch along with CFST column specimens. Modulus of elasticity and Poisson's ratio test were performed on three cylinders in each batch at 28 days and then the cylinders were loaded up to failure to get the compressive strength. The Modulus of Elasticity of concrete was also measured during crushing strength test of each representative cylinder. The average compressive strength of all three cylinders is found 20.25MPa. The average Value of Modulus of elasticity and Poisson's ratio were 16859MPa and 0.217.

4. EXPERIMENTAL TEST SETUP

All tests were conducted using a Universal Testing Machine (UTM) that has a loading capacity of 2000kN. The upper head of the UTM was moveable and the compression load was applied by the lower ram. Total four LVDT transducers and a load cell were attached to the CFHS test specimens. An UCAM60B type data logger with a computer connection was used for the acquisition of test data. A schematic diagram of test setup and data acquisition system is shown in Figure 2. Two bearing plate of thickness 12mm were placed at the top and bottom of the CFST test specimens to ensure the uniform loading. Two spirit level were used for centering the test specimen to ensure the concentrically applied axial loading. Test setup and instrumentation for CFST test specimens are shown in Figure 3.

The test specimens were placed under the UTM to provide uniform loading having top end of the specimen was fixed as the loading ram moves upward. Three Linear Veriable different transducer (LVDT) were set at the middle height of the specimen to acquire the lateral deformation of the CFHS specimens. Similarly, one LVDT transducer was attached at the upper head of the UTM to acquire the axial deformation of the test specimens. Load cell was placed at the bottom of the test specimen and on the loading ram. The capacity of LVDT transducers varies from 25mm to 100mm and the load cell of 2000kN. Axial load application rate to the test specimens varies from 5kN/sec to 0.5kN/sec because the UTM was analog and operated manually. The loading rate was high (5kN/sec.) at the Initial level and low (0.5kN/sec.) after the peak load. All the data was recorded and stored using data logger and laptop.

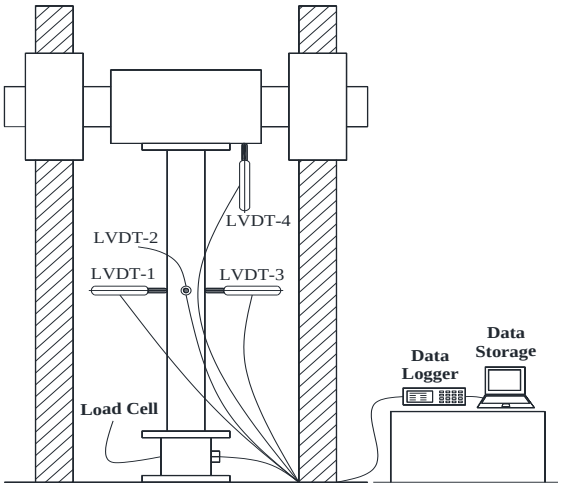

Figure 2: Schematic Diagram of Test Setup and Data Acquisition System

Figure 3: Test setup and instrumentation for CFST columns in laboratory

5. EXPERIMENTAL RESULT AND DISCUSSION

The variable is considered in the test program was b/t ratios along with L/b ratio of cross-sectional dimensions and concrete mix ratio of 1:1½:3. The loads were applied concentrically from the bottom of the column specimens. The experimental load-deformation behavior, peak load, peak strain and failure modes of the specimens were examined. The specimen designation, strength of representative concrete cylinder and steel plate along with peak load and corresponding strain are listed in Table 2. The load versus deformation relation of CFST test specimens, failure pattern etc. are presented in this section.

5.1 Axial load versus Axial Deformation Relation of CFST Columns

Three groups of specimens were tested under concentric axial load to observe the load versus axial deformation behavior of CFST specimens. Axial load and axial deformation were recorded for each column specimens experimentally. Load-deformation curves are drawn and shown in Figure 4. From Figure 4, it can be clearly seen that the axial load carrying capacity is increased corresponding to decrease the axial deformation with the increase and b/t ratio. Shanmugam et al. (2002) and Yuan et al. (2019) reported that the axial capacity of concrete filled tube was increased with the decrease in b/t ratios.

5.2 Failure Modes, Peak Load and corresponding Strain of CFST Columns

Nine CFST column specimens in three different groups were tested under concentric axial load. Three similar specimens of the same conformation are being considered in each group. The failure pattern was almost same in all specimen groups. Even at peak load, no failure mode has been observed. After peak load, failure pattern of the test specimens has been observed at large deformation. Local buckling with outward bulging were observed near the loading or support end in steel tube of CFST column specimens during experimental investigation. The point of ultimate failure was visually characterized by the yielding and buckling of steel tubes. The peak strain of each specimen was calculated from peak deformation corresponding to peak load. Experimental peak loads and corresponding strains of CFST specimens are given in Table 2.

Table 2: Experimental Peak Load and corresponding Strain of the CFST Specimens

Sl. No	Specimen **Designation**	Compressive Strength of Concrete f_{cu} **(MPa)**	**Strength of steel plate of HST** f_y **(MPa)**	f_u **(MPa)**	Peak Load $P_{expt,}$ **(kN)**	Strain at Peak Load ε_{Expt} ($\mu\varepsilon$)
1	**FRB-18-10**	**20.25**	**309**	**365**	**153.5**	**13129**
2	**FRB-25-10**	**20.25**	**309**	**365**	**168.0**	**10680**
3	**FRB-35-10**	**20.25**	**309**	**365**	**240.0**	**10229**

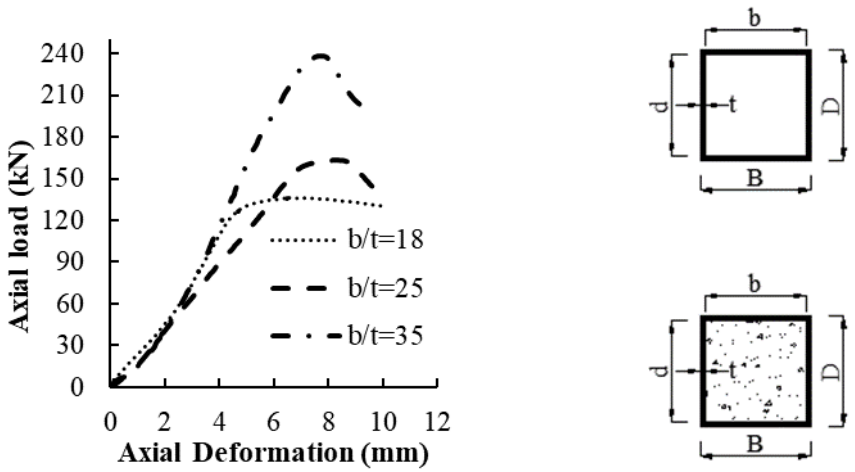

Figure 4: Load versus Axial Deformation curve of Specimens having different b/t Ratios

6. FINITE ELEMENT ANALYSIS

The Finite Element Method (FEM) is a powerful technique employed in engineering and structural analysis to simulate the complex behavior of structures. Finite Element (FE) Analysis of CFST column specimens is done under concentric loading. The material properties used in numerical simulation are shown in Table 3. Three columns are numerically modelled and analyzed using ANSYS FE code for concentric axial load.

6.1 Elements Considered of Finite Element Model

A 3D finite element model was developed in this study to investigate numerically the behavior and strength of CFST specimens considering geometric and material properties. Both geometric and material nonlinearities were incorporated in the FE model. ANSYS 2021R2 finite element code were used to develop the nonlinear FE model of CFST specimens.

Table 3: Material Properties of Steel Plate and Infill Concrete

Specimen Designation Group	Properties of Concrete			Properties of Steel Plate		
	f_{cu} (MPa)	E_c (MPa)	Poisons's Ratio, ν	f_y (MPa)	f_u (MPa)	ε_u (%)
FRB-18-10	20.26	16859	0.217	309	365	21.5
FRB-25-10	20.26	16859	0.217	309	365	21.5
FRB-35-10	20.26	16859	0.217	309	365	21.5

The CFST columns investigated in this study comprised of two components, viz. hollow steel tube (HST) and infill concrete. The HST in CFST column was modeled with **SOLID185** element as shown in Figure 5. Each node of the SOLID185 element has three degrees of freedom: translations in the nodal x, y, and z directions. The concrete of CFST column was modeled using **CPT215** element. Only difference from SOLID185 is the number of degrees of freedom. The CPT215 element has eight degrees of freedom in each node: translations in the nodal x, y, and z directions, pore-pressure, temperature and nonlocal field values. The element also has elasticity, stress stiffness, large deflection, and large strain capabilities. Bonded contact was used in between HST and infill concrete of the CFST column specimens.

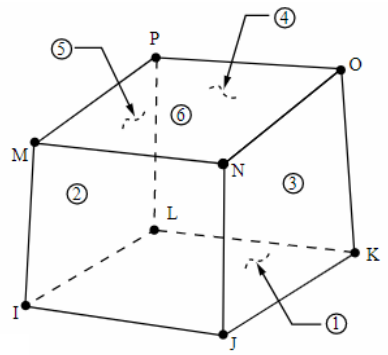

8-node solid element

Figure 5: Elements (SOLID185/CPT215) Considered in the Numerical Simulation

6.2 Modelling of Steel-Concrete Interactions

The HST and infill concrete interfaces are modelled as bonded type contact element. In modeling of CFST columns, the outer surfaces of infill concrete were defined as contact surface whereas the inner surfaces of steel tube were defined as target surface as shown in Figure 6. When bonded contact is applied in between two surfaces in ANSYS FE, it means the surfaces are glued to each other. When displacement or force was applied on infill concrete, it was expanded due to its Poisson's effect. The confinement of infill concrete would reduce by this phenomenon. Two bearing plates were also used at the top and bottom ends of the CFST column to conform the uniform loading on both steel tube and

infill concrete. The contact properties of these bearing plates and CFST column were defined as frictionless and adjust to touch for interface treatment to avoid complexity in solution strategy.

6.3 End Boundary Conditions

The boundary conditions in the FE model were defined in such a way to comply with that applied in the experimental setup. The boundary conditions applied in the FE model to simulate the conditions of CFST column specimens are shown in Figure 7. The top end of the column was fixed and the axial load was applied through rigid body reference node at the center of the bottom end of the column.

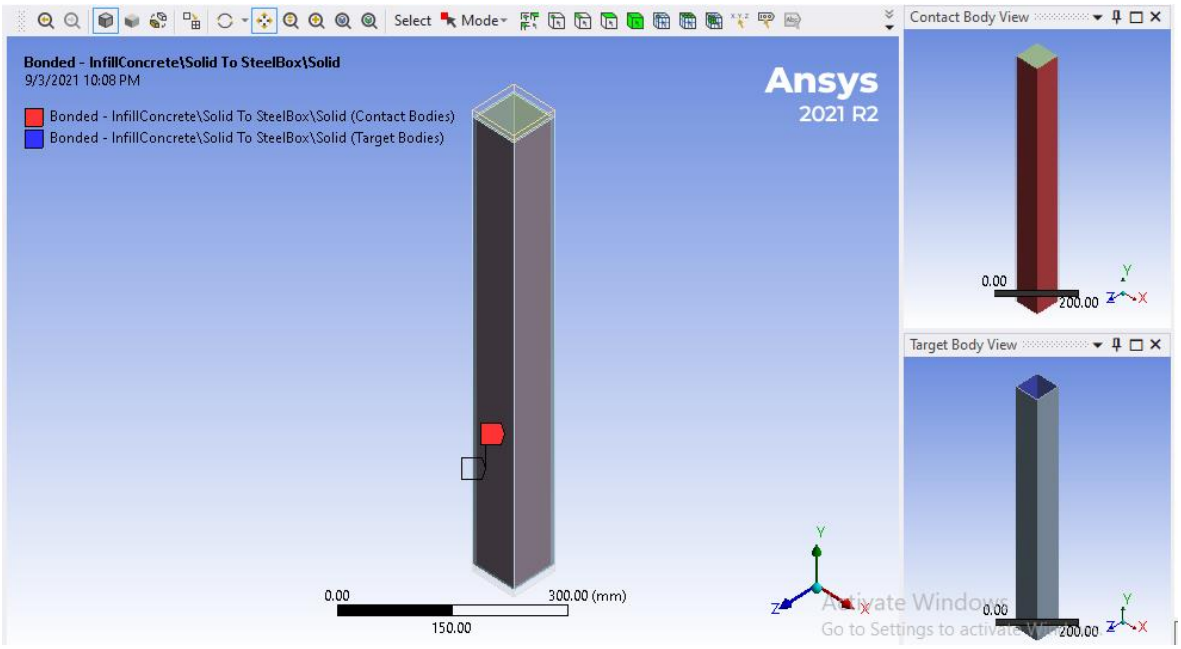

Figure 6: Contact Regions of CFST column

6.4 Performance of Finite Element Model

The predicted load versus deformation response, peak load, peak axial strain and failure modes obtained from the finite element analysis for each of the CFST column specimens are compared with the corresponding experimental results of the current study. The comparison between numerical and experimental results in terms of deformation, axial capacity, axial strain at peak load and failure modes are described in the succeeding sections.

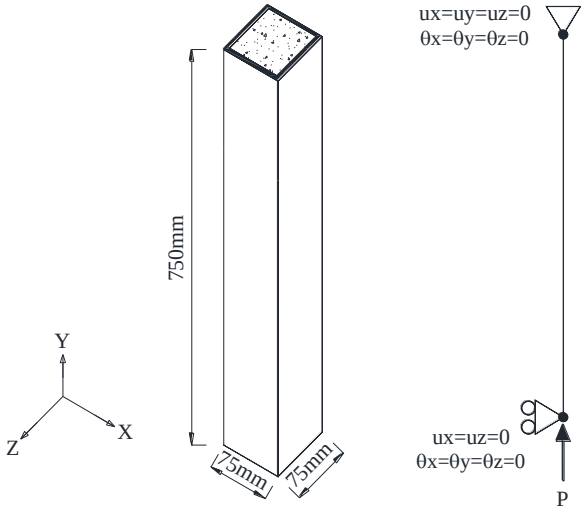

Figure 7: End Boundary Condition in FE Model

6.4.1 Axial Load versus Axial Deformation

Experimental load versus deformation curves are compared to the same obtained from finite element analysis for each group of specimens. The comparison between the experimental and numerical load versus deformation curves for specimen groups FRB-18-10, FRB-25-10 and FRB-32-10 having same L/b (=10) ratio and concrete mix ratio (1:1½:3) with different b/t ratios are shown in Figure 8. The abscissa is defined as axial deformation and ordinate is defined as axial load.

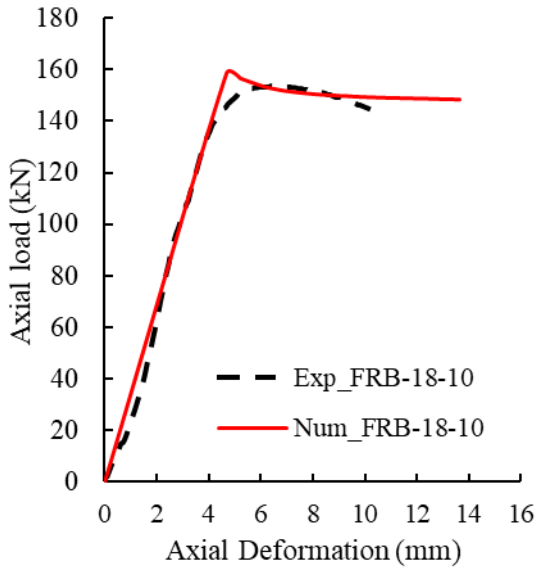

(a) FRB-18-10

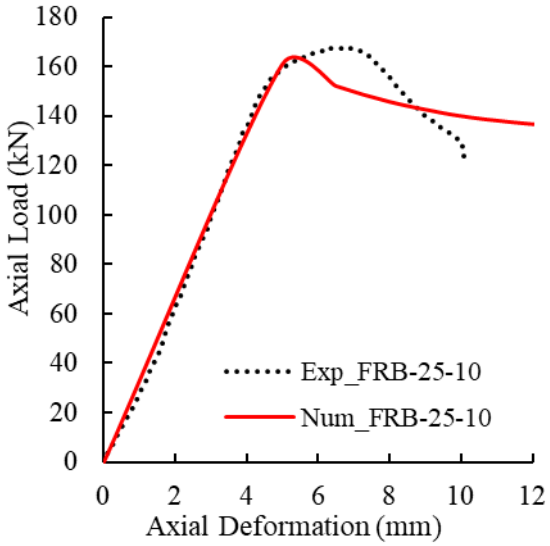

(b) FRB-25-10

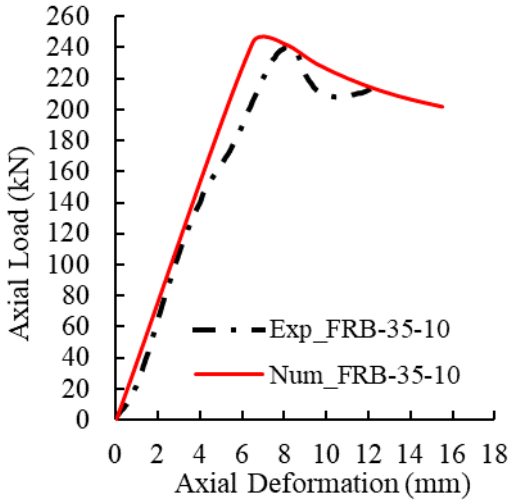

(c) FRB-35-10

Figure 8: Load versus Deformation Relations

The load versus axial deformation curves obtained from the numerical analysis were found to be good agreement with the experimental curves up to the peak load. The ascending branches of the numerical load-deformation curves are almost similar to the ascending branches of the experiments load-deformation curves. The descending branches of numerical load-deformation curves have found a little bit deviated from the descending branches of experimental load-deformation curves of these three groups of column specimens. This variation may be attributed to the variability in the concrete casting and residual stresses of steel tubes in the experimental work. The recession limb of numerical load-deformation curve goes upward than experimental load-deformation curves because infill concrete is considered to be hardened after being dilated at large deformation.

6.4.2 Axial Load and Axial Strain at Peak Load Level

Nine CFST column specimens were tested under concentric axial load in this study work. The experimental peak load and corresponding strain were compared inTable 5Table 5 to the numerical peak load and corresponding strain obtained from finite element analysis conducted for the test specimens. The ratio of numerical-to-experimental peak load (P_{Num}/ P_{Expt}) for the test specimens varied from 1.0 to 1.03 with a mean value of 1.02 and standard deviation of 0.018. This indicates that the performance of the finite element model in predicting the ultimate capacity of the test columns is well. Table 5 shows the mean ratio of numerical-to-experimental axial strain at peak load (ε_{Num}/ ε_{Expt}) was 0.917 with a standard deviation of 0.015. Although providing good estimation of peak load, the numerical model is observed to underestimate the axial strain at the peak load. This difference could be due to the presence of geometric or load imperfections and the variability in concrete properties in the test specimens.

Table 5: Numerical and Experimental Peak Load and Corresponding Strain

Sl. No.	Specimen Designation	Peak Load Capacity (kN)		P_{Num}/ P_{Expt}	Axial Strain at Peak Load		ε_{Num}/ ε_{Expt}
		P_{Num}	P_{Expt}		ε_{Num} ($\mu\varepsilon$)	ε_{Expt} ($\mu\varepsilon$)	
1	FRB-18-10	158.54	153.18	1.03	11968	13129	0.91
2	FRB-25-10	167.89	167.83	1.00	9971	10680	0.93
3	FRB-32-10	243.40	240.09	1.01	9266	10229	0.91

Mean	**1.02**	**0.917**
SD	**0.018**	**0.015**

6.4.3 Modes of Failure

In the test CFST column specimens, the primary mode of failure was yielding and local buckling of steel tube. At the peak load, no failure modes were physically observed. The appearance of yielding of steel tube was observed after the peak load when large deformation occurred with less decreasing of axial load. The local buckling of steel tube was observed at upper and lower one-third (L/3) length of the test columns.

The failure modes for CFST columns were identified from the finite element analysis and compared with the failure modes in the experiments. The failure modes were plastic damage or dilation of infill concrete followed by yielding and local buckling of steel tube. These two modes were identified by examining the stress of the infill concrete and steel tube elements at a large deformation after the peak load. A comparison between the numerical and experimental failure mode of the test columns are shown in Figure 9. In both cases failure was initiated by dilation of infill concrete followed by yielding and local buckling of steel tube.

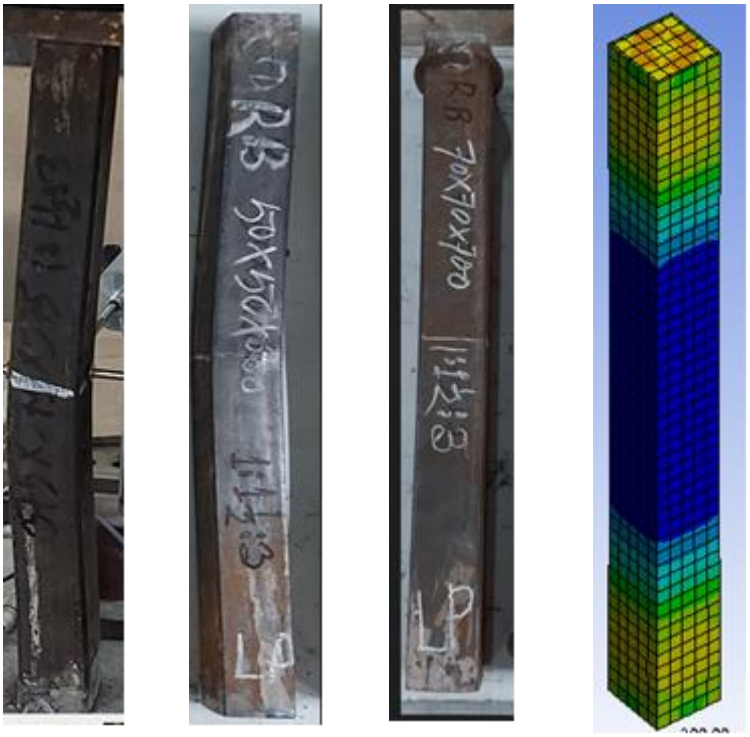

(a) Experimental (b) Numerical

Figure 9: Failure Mode of Columns FB1-25-6, FB1-28-10 and FB3-25-10

7. CONCLUSIONS

The following conclusions may be drawn based on limited experimental investigation as well as numerical simulation of the test specimens are summaries below:

(i) The axial capacity of CFST column specimens increased with decreasing the axial deformation when the b/t ratios are increased with constant L/b ratio and concrete strength;

(ii) The typical failure modes of recycled brick aggregate CFST columns are found similar to those of the virgin brick CFST columns. Bulging failure patterns were observed.

Therefore, recycled brick aggregate CFST columns offer an innovative and eco-friendly approach tostructural design of composite column, supporting the transition towards a more sustainable andresource-efficient construction industry.

ACKNOWLEDGEMENTS

The authors acknowledge their sincere gratefulness to the Department of Civil Engineering, Dhaka University of Engineering & Technology, Gazipur, for the support and cooperation to conduct the experimental as well as numerical research work. Without the endless support, this work would not have been finalized.

REFERENCE

Neogi, P. K. (1967). *Concrete Filled Tubular Columns*. In *Imperial College of Science and Technology, London.*

Ge, H., and Usami, T. (1992). *Strength of Concrete-Filled Thin-Walled Steel Box Columns*: Experiment. *Journal of Structural Engineering(ASCE), 118(11), 1233–1250*.

Ge, H., and Usami, T. (1994). *Strength analysis of concrete-filled thin-walled steel box columns*. Journal of Constructional Steel Research, 30(3), 259-281.

Schneider, S. P. (1998). *Axially loaded concrete-filled steel tubes*. Journal of Structural Engineering (ASCE), 124(10), 1125–1138.

Huang, C. S., Yeh, Y. K., Liu, G. Y., Hu, H. T., Tsai, K. C., Weng, Y. T., Wang, S. H., and Wu, M. H. (2002). Axial Load Behavior of Stiffened Concrete-Filled Steel Columns. Journal of Structural Engineering, *128*(9), 1222–1230.

Shanmugam, N. E., Lakshmi, B., and Uy, B. (2002). *An analytical model for thin-walled steel box columns with concrete infill*. Engineering Structures, 24(6), 825–838.

Yang, You-Fu and Han, Lin-Hai (2006), *Compressive and flexural behavior of recycled aggregate concrete filled steel tubes (RACFST) under short-term loadings*. Steel and Composite Structures, Vol. 6, No. 3, pp. 257-284.

Chen, C. C., J. W. Ko, G. L. H., and Chang, Y. M. (2012). *Local buckling and concrete confinement of concrete-filled box columns under axial load*. Journal of Constructional Steel Research, 78(6), 8–21.

Xiao, J. Z., Huang, Y., Yang, J., and Zhang, C. (2012). *Mechanical properties of confined recycled aggregate concrete under axial compression*. Journal of Construction and Building Materials, 26(1), 591–603.

Schwerin, D. E., Cavalline T. L., and Weggel D. C. (2013) *Use of Recycled Brick Masonry, Aggregate and Recycled Brick Masonry Aggregate Concrete in Sustainable Construction*. KICEM Journal of Construction Engineering and Project Management.

Mohammed, T. U., Hasnat, A., Awal, M. A., and Bosunia, S. Z. (2015). *Recycling of Brick Aggregate Concrete as Coarse Aggregate*. Journal of Materials in Civil Engineering, *27*(7). https://doi.org/10.1061/(asce)mt.1943-5533.0001043.

Akhtar, A., and Sarmah, A. K. (2018), *Construction and demolition waste generation and properties of recycled aggregate concrete: A global perspective*. Journal of Cleaner Production, 186, 262-281.

Yuan, F., Huang, H., and Chen, M. (2019). Behavior of square concrete-filled stiffened steel tubular stub columns under axial compression. Advances in Structural Engineering, 22(8), 1878–1894.

Ahmed, H., Tiznobaik, M., Huda, S.B., Islam, M.S. and Alam, M.S. (2020). *Recycled aggregate concrete from large-scale production to sustainable field application*. *Construction and Building Materials, 262, paper No.-119979.*

G. Pandulu, R. Jayaseelan and M. Priya (2020), *Application of Recycled Coarse Aggregate in Steel Tubular Members*, Nature Environment and Pollution Technology, Vol. 19, No. 2, pp. 729-737.